High-temperature deformation in bulk polycrystalline hafnium carbide consolidated using spark plasma sintering

D. Demirskyi (a,b,c)†, O. Vasylkiv (b)†, and K. Yoshimi (c).

(a) Advanced Institute for Materials Research (AIMR), Tohoku University, 2-1-1 Katahira, Aoba-ku, Sendai, 980-8577 Japan
(b) National Institute for Materials Science, 1-2-1 Sengen, Tsukuba, Ibaraki 305-0047, Japan
(c) Department of Materials Science and Engineering, Tohoku University, 6-6-02 Aramaki Aza Aoba, Sendai, 980-8579, Japan

Abstract

In this study, we report the three-point flexural strength and fracture toughness of monolithic hafnium carbide up to 2000 °C. HfC with different grain sizes was consolidated using the spark plasma sintering method. Coarse-grained monoliths showed a weak dependence on the strain rate during high-temperature tests at 1600 °C–2000 °C. In contrast, results for the ceramics with a grain size below 20 μm indicated a positive dependence of the yield strength vs strain rate. This allowed us to identify the activation energy for high-temperature deformation in flexure as 370 kJ/mol. This level of activation energy is in satisfactory agreement with reports about the diffusion of C in hafnium carbide.

Keywords: hafnium carbide; grain size; flexural strength; high-temperature materials.

1 Introduction

The design of next-generation hypersonic flight vehicles has raised interest in the development of materials that can operate in extreme environments. Under such conditions, thermal protection structures are required to operate in air/vacuum at temperatures that can exceed 2000 °C, thus components are not only required to have very high melting points, but also oxidation and ablation resistance. From the vast array of structural materials, there is a limited number of materials (compounds and elements) that meet requirements for the described working conditions in which the so-called ultra-high temperature ceramics (UHTCs) are included [1]. Typically, the group IVB and VB bulk carbides, nitrides, and borides belong to the UHTCs family. Monolithic transition metal carbides act as a backbone for the UHTC family [2–4], as HfC–TaC [5,6], for instance, have the highest reported melting point for any compound. Recently, there has been much particular attention paid to the high-entropy ceramics or high-entropy carbides [7–9]. As mentioned for the HfC–TaC system, some extreme properties can be explored and potentially utilized for other members of the UHTC family. Having said that, in [7], it has been noted that only selected studies have reported the strength properties of HfC [10–13]. This is thought to be due to its high-melting point (3900 °C), and thus the unavoidable presence of HfO_2 during consolidation at extremely high temperatures [13,14]. Nevertheless, it

was analyzed that in some instances HfC bulks showed an increase in strength with an increase in temperature, suggesting that microplastic deformation is being activated in this relatively brittle metal carbide [13].

This provides the potential of being used at temperatures approaching 2000 °C, however, essentially the low diffusivity in the monolithic UHTCs in general [15], and for HfC in particular, indicates that processing of the bulk additive free HfC [13,14] remains a challenge. In order to produce highly dense monolithic hafnium carbide in this study, we used a commercial Zr-free HfC and employed spark-plasma sintering to promote densification [7–9, 16].

This study, for the first time, explores the microstructure evaluation during multiple sintering runs of HfC, which have been made in order to determine the flexural strength, hardness, toughness and Young's modulus. Flexural strength at elevated temperatures was evaluated for HfC bulks with different grain sizes. High-temperature deformation in flexure was evaluated for specimens which have a strong correlation between the strain rate and yield strength at 1800 °C–2000 °C.

2 Materials and Methods

Commercially-available HfC powder (Alfa Aesar, Lot #W19E52), which consists of micrometer aggregates of sub-micrometer ~300 nm crystallites was used as the starting material. The received untreated powder was used for consolidation using

the spark plasma sintering (SPS) method. The SPS experiments were conducted using the 'Dr. Sinter' 1050 (Sumitomo, Japan) unit with a 30-mm die, as a rule, 20 to 25 g batches were used.

The schedule for the hafnium carbide specimens prepared in this study had four major steps: (1) heating to 900 °C in four minutes following (2) a 50 °C/min heating to densification temperature within the 1600 °C to 2100 °C range. The dwell between 1 and 20 minutes at the densification temperature was used. The third step included cooling to 600 °C in 20 minutes. The pressure of 32 kN was maintained during the consolidation and cooling stages. Argon gas at the flow rate of 2 L/min was used.

An X-ray diffraction (XRD) analysis (D8 Advance, Bruker, Karlsruhe, Germany) was performed on the polished surfaces of the bars after the flexural tests using Cu-Kα radiation. The intensity data were collected over the 2θ range of 20°–145°, in steps of 0.02–0.05° using a sampling time of 10 s for each step. The software used for refinement was TOPAS (TOPAS Ver. 4.2, Bruker AXS, Germany). Instrumental broadening was determined using a NIST 660b LaB_6 standard run under the same conditions for each carbide sample.

The structural characteristics of the hafnium carbide ceramics were studied using scanning electron microscopy (SEM, JCM-6000, JEOL) with secondary (SE) or backscattered electrons (BSE mode).

The three-point flexural strength was determined using rectangular blocks (2×2×25, 2×2.5×25 mm) and the strength testing equipment were previously described in detail [17]. A span of 16 mm was used. The fracture toughness of the ceramics was evaluated by the specimen bending testing which contained a single edge through-thickness notch following ASTM C1421–10. Details of the testing configuration and the notch profile are presented in ref. [18]. We evaluated the elastic modulus (Ef) for the tests from the linear portion of the load-displacement curve using the procedure described in ASTM E111–04 [19].

To evaluate the strain dependence of the yield stress [20] for the hafnium carbide, tests were performed using loading rates of 0.1 to 25 mm/min (1600 °C–2000 °C) and low temperature tests were performed at the loading rate of 0.5 mm/min. Tests at elevated temperatures were performed in argon.

The hardness was determined by an MMT-7 Vickers hardness tester (Matsuzawa MMT-7; Matsuzawa SEIKI Co., Ltd., Tokyo, Japan) using a load of 9.8 N and 98 N with a dwell time of 15 s following the standard procedure (ASTM C 1327–15).

3 Results and Discussion

3.1 Phase analysis of hafnium carbide bulks

X-ray studies revealed that the lattice parameters of hafnium carbide varied between 4.6399 Å and 4.6414 Å for the powder and bulk, respectively. The initial powder

showed only peaks of Hf and C during EDX, while faint peaks of O and Nb (~0.2 mol.%) were noted. Traces of other metals in the powder or consolidated HfC bulks have not been identified. The XRD results revealed that the majority of the bulk specimens (within >80 measurements) can be refined using the lattice parameter of a = 4.640±0.002 Å (**Figures 1,2**). Traces of free carbon ((002) peak at 26.5°) were seldomly observed even for the mirror-polished specimens. The minor presence of cubic oxide was rarely identified using the (200) peak and lattice parameter of 5.14±0.01 Å. Based on the lattice parameter, the X-ray density was evaluated as 12.66 g/cm^3. The porosity was identified by SEM using a polished specimens and FIJI software [21]. The bulk density was measured using Archimedes method, and neither of the specimens, including those with a porosity below 0.02% by an SEM analysis approached the number. According to the reference literature, the theoretical density of HfC is 12.20 g/cm^3 [2,4,15]. However, this value appears to be an underestimation, as one can see from **Figure 3** that the bulk density of the fully dense material was 12.40 g/cm^3 (97.9% of X-ray density). For this study, the value of 12.40 g/cm^3 was accepted as the theoretical density (TD) for evaluation of the relative density. Similar value has been used in [22].

3.2 Densification and grain growth of hafnium carbide

Figure 4 illustrates data of the mean grain size as a function of the relative density. One can see that only a slight coarsening was observed below 75 % TD (see **Figure 5**), while grain growth followed an exponential dependence after a threshold density of 97% was achieved. Large grains, up to 100–200 μm, were frequently observed for the specimens after SPS above 2000 °C. One should bear in mind that the original powder was prepared by a wet chemical method and was not milled. The powder consisted of crystallites of ~300 nm assembled into 1 to 6 μm aggregates.

Hence, the raw hafnium carbide powder acted as the initial source of porosity due to the porosity that originated from the original aggregates [23]. As a rule, this porosity is difficult to remove during processing (**Figure 6**), as such pores are entrapped in the original large aggregates (up to 6 μm).

For most hafnium carbide specimens before reaching an ~15 μm grain size, pores were located on the grain boundaries, while for the coarser grains pores were located mostly inside the grains. These pores had a size between 1 and 2 μm and a spherical shape, which are indications of the closing of the pore channels during the intermediate stage of sintering [24]. Despite lengthy dwells up to 20 min at 2100 °C, these pores cannot be eliminated during solid-state sintering [25], as at temperatures exceeding 2000 °C, the grain growth would dominate over densification. An exception would be promotion of the recrystallization during high-temperature annealing, however such, reports are rather scarce for carbides [26]. In addition to

grain growth SPS at temperatures exceeding 2000 °C, it would result in the minor presence of an oxide phase (black in BSE mode) in quantities up to 0.3 vol.%. For polished specimens, the oxide is often located mainly between two adjunct grains in the form of a fiber. Such an example is highlighted by the arrows in **Figure 6 (g)**. No oxide grains were observed for the fine-grained materials or bulks consolidated below 2000 °C.

From a wide spectrum of possible specimen data we selected four ceramics with different grain sizes that are labeled as grades A, B, C and D in **Figure 4**. Representative microstructures for the polished specimens and following flexural tests at 2000 °C are presented in **Figure 6**.

3.3 Mechanical properties of HfC ceramics

The macroscopic hardness for bulk polycrystalline ceramics were reported in several studies [2,4,13,22,27–32]. However, the majority of the tests presented in the reference books were obtained using micro-loads from 50 to 200 g-force (0.49 N to 1.96 N). **Figure 7** summarizes the hardness measurements collected within the present study. In general, with a load exceeding a 9.8 N hardness, the hafnium carbide has a slight scattering between the different grades tests. However, at 98 N, the hardness can be averaged as 15.2±1.6 GPa. This provisional value is in good agreement with the data of Silvestroni et al. [13].

The fracture toughness determined using notched specimens in flexure varied within 2.2±0.4 MPa $m^{1/2}$ for all the tested specimens. The exception was grade D, with the coarsest grain size, as these ceramics had a slightly lower measured fracture toughness (1.6±0.1 MPa $m^{1/2}$). Furthermore, attempts to check the variation in the fracture toughness for grade D at elevated temperatures between 1600 °C and 2000 °C indicated that the toughness remains constant up to 2000 °C at which a value of 1.9 MPa $m^{1/2}$ was measured.

The flexural strength showed a noticeable resemblance to the Hall-Petch relation and varied between 300 and 600 MPa (**Figure 8**). The data of ref. [13] are provided as a visual reference. Specimens with a relatively high porosity level between 10 to 15 % showed a strength of 406±32 MPa, while the highly-porous specimens with a density of 72 to 78 % TD showed strength of 118±6 MPa.

Attempts were made to evaluate the bulk's Young's modulus of the hafnium carbide obtained by flexure. First, the data were collected and the porosity has been identified from the SEM of the top surface of every individual bar after flexure. It is known that the elastic moduli are quite sensitive to the porosity level [33], and there are several functions that can describe the mechanical properties as a function of porosity. We selected a simple exponential function in order to identify the porosity of the pore-free HfC (**Figure 9**). The modulus of 426 GPa was obtained from such an analysis. Several individual tests showed slightly higher values of Young's

modulus, hence, 426±10 GPa can be considered as a provisional result. The data are in good agreement with values reported in [13],[15]. However, ref [31], indicated that the values of 750 GPa can be considered in engineering calculations. Based on results of this study, we consider such a value as an overestimation (data were derived from highly porous specimens). Data of ref [22] 360±29 GPa for 98.5 % TD monolithic HfC are too low, as such values were evaluated for specimens with a ~15 % porosity in this study.

Figure 10 illustrates the change in Young's modulus with temperature for grade D. Noticeably, all the recorded curves for these ceramics only had a linear elastic part even at 2000 °C, the data of refs. [31,34–36] illustrate trends in Young's modulus change with temperature for HfC and ZrC.

3.4 High-temperature deformation behavior

Figure 11 illustrates the temperature dependence of the strength of the hafnium carbide bulks prepared in the present study and previously reported flexural tests results [10–13]. It is worthy to note that for coarse grained ceramics, i.e., grades C and D, only a minor difference in the strength at the different temperatures was observed. Furthermore, the flexural strength data can be approximated by a quasi-linear relationship as presented in **Figure 11** using the dotted lines for the 95% confidence intervals.

The data for hafnium carbide ceramics with finer grains resulted in different shapes of the strength vs temperatures curves. Grade A, hafnium carbide with the finest grain size, showed a steadily decline in the strength versus temperature, which became more clear after the 1600 °C tests. That being said, the strength at 1000 °C was considerably higher than for the coarser grade C or grade D (400 vs 300 MPa). Grade B showed a very strange behavior as the strength increased up to 1600 °C, followed by a rapid decline up to 2000 °C. This behavior has been previously observed for carbide ceramics [7,9], and can be explained as follows. The increase in strength can be attributed to the ongoing microplastic deformation inside the HfC grains despite the fact that the loading curves for these ceramic bulks were linear before fracture.

At temperatures exceeding 1600 °C an intergranular fracture becomes the dominant fracture mechanism. Such change in the macroscopic fracture mechanism, as a rule, leads to a decrease in strength [37]. However, as one can see from the data or ref. [10], the strength may further increase, which can be understood by the accommodation of plastic deformation inside the grains and activation of the grain sliding [3]. Based on results of this study, is that the grain sliding contribution should decrease with the larger grains, hence slightly higher strength were observed for coarse grains.

In order to obtain additional high-temperature deformation data of the monolithic hafnium carbide specimens, we attempted to determine the yielding behavior of the SPSed highly-dense HfC at different strain rates. Previously, it has been mentioned that different carbide ceramics may have a different dependences on the strain rate [20,38]. Most noticeably, Darolia and Archbold [20] reported that for polycrystalline zirconium carbide, a positive variation of 0.2 yield strength may allow one to estimate the activation energy for the carbide at elevated temperatures.

Using the methodology proposed in [20], we attempted this approach for hafnium carbide with different grain sizes. **Figure 12** shows the dependence of the yield strength of the grade A carbide as a function of the strain rate at 1800 °C, 1900 °C and 2000 °C. The **Figure 12 (c)** shows the dependence of the yield strength of the HfC carbide as a function of the strain rate at 2000 °C for grade A for selected strain rates. For clarity we show only one full strain-stress curve is presented. The data on the 0.02 yield strength can be approximated using a linear regression with the inverse slope values between 4 and 5. In contrast, that hafnium carbide bulks with a grain size exceeding 25 μm had a weak strain rate dependence (grade C), or the strain rate did not affect the yield point for the attempted strain rates (grade D, **Figure 13**). The analysis of grade B is in general agreement with the data of ref [20]. As a result, the values were observed in [20], which are provided as a reference in **Figure 14**. As noted by Kelly and Rowcliffe for TiC [38], and by Darolia and Archbold [20] for

ZrC, one can quantitively calculate the activation volume for the strength-related tests at elevated temperatures as:

$$V = kT\frac{\Delta \ln \dot{\varepsilon}}{\Delta \sigma}.$$

where the k is the Boltzmann constant, T is the absolute values of the temperature of the test, $\dot{\varepsilon}$ is the plastic strain rate, and σ is the yield strength. The activation volume can be obtained by plotting the yield strength vs logarithm of the strain rate (**Figure 14**), which yields values of 368 $Å^3$ and 352 $Å^3$ at 1800 °C and 2000 °C, respectively. The data for ZrC [20] presented in **Figure 14** would yield 373 $Å^3$ at 1800 °C. Assuming the lattice parameter from the XRD measurements as 4.64 Å, one can expect that such a volume is proportional to ~30$\boldsymbol{b^3}$ ($\boldsymbol{b}$ is a a/2 [1-10]). For clarity, the tantalum carbide values of 50$\boldsymbol{b^3}$ to 55$\boldsymbol{b^3}$ have been reported [39].

Knowing both the yield strength and activation volume allows one to estimate the activation energy for the high-temperature deformation from the plot of ($\ln \sigma + \sigma V/kT$) versus 1/T. Such efforts results in the activation energy of 370±15 kJ/mol. **Table 1** summarizes the creep and diffusion data by various methods for HfC and ZrC [20,40–42]. Based on the values of the activation energy, one can presume that similar to other carbides, these values may indicate that the diffusion of carbon in metal (metal carbide) is the rate limiting process. Nevertheless, one cannot underestimate the proximity of the activation energy reported in this study and that reported by Zubarev for ZrC [20] (370 kJ/mol, and 368 kJ/mol, respectively).

Although studies [20] and [3] indicate the same mechanism, one can note the difference in the activation energy (368 kJ/mol [3], 501±19 kJ/mol [20]), which can be explained by a different temperature range, grain sizes, carbon deficiency, or loading methods (constant loading in [3]).

We emphasized that hafnium carbide bulks with grain sizes exceeding 25 μm prepared from the same raw powder showed that the loading rate did not affect the yielding at elevated temperatures. In fact, for grade D (**Figure 15**), high-temperature fracture was identical above 1600 °C. Considering the intergranular fracture as the main mechanism at elevated temperatures, one can expect the strength of 350±15 MPa for grades C, D is the strength of the grain boundaries at elevated temperature. This strength shows how good grains of HfC are sintered together using SPS. One can see that grades A or B after the flexural tests show a strength smaller than coarser grains (**Figure 11**). One should mind that temperature/dwell for the consolidation of grade D and A were 2100 °C/15 min and 1840 °C/6 min, respectively. Hence, one may expect that specimens consolidated at a longer dwell will have a better performance at elevated temperatures. In terms of possible practical applications at elevated temperatures, where plastic deformation should be somehow avoided or limited [3], hafnium carbide ceramics with coarser grains and elastic fracture at 2000 °C may be recommended.

Based on the theoretical viewpoint, the high-temperature strength behavior can be directly connected to the grain size, as similar observations has been made for Al_2O_3 [43], UO_2 [44], and ZrC [3]. Although in each individual case a different mechanism may contribute, the general observation that may clarify the results for HfC is that the grain sliding contribution should decrease with the larger grains; same is true for the consolidation of coarse powders.

Canon et al. [44] summarized that a decrease in strength at elevated temperatures can be directly attributed to grain-boundary sliding, while the rate-controlling mechanism for the grain deformation would be caused by dislocations. As noted by Coble [45] in his discussion about deformation of oxides, the thickness affected by dislocations may be considered as 10^2–10^4 Å (0.01 to 1 μm). As expected, if the grain size being an order of magnitude larger than the apparent widths of the boundaries (or thickness within which diffusion is enhanced), it can be expected that grain-boundary diffusion should be rate controlling. The data of Zubarev [3] summarized in **Table 1** for HfC and ZrC are for 11 μm and 14–30 μm, respectively. Hence one can view the grain size as a factor contributing to the resistance to deformation is [3,41,46–48]. For carbides the grains coarser than 15 μm as in [46–48] would mean that the bulk (lattice) diffusion mechanisms will be dominant and the contribution of the grain-boundary diffusion would be minimal. Andrievskii et al. [41] suggested that based on the diffusion profiles of ^{14}C in carbides, the

contribution of the grain-boundary diffusion was at the detection limit during the creep tests above 2200 °C. Hence, the activation energy evaluated for the high-temperature deformation tests in flexure indicated the rate limiting process should be that of carbon in the carbide.

Conclusions

In summary, hafnium carbide bulks consolidated using spark-plasma sintering despite possessing a high brittleness (fracture toughness 2.2 MPa $m^{1/2}$) and relatively high hardness of 15 GPa, show an adequate level of flexural strength (up to 600 MPa). The room temperature flexural strength followed a Hall-Petch like dependence suggesting that a higher strength can be further obtained after mastering the densification and grain growth. Coarse grained monoliths showed a weak dependence on the strain rate during high-temperature tests at 1600 °C–2000 °C. The results for ceramics with a grain size below 20 μm indicated a positive dependence of the yield strength vs strain rate. This allowed us to evaluate the activation energy for high-temperature deformation of 370 kJ/mol which is comparable to previous reports on HfC and ZrC ceramics.

Acknowledgements

Authors express their sincere appreciation to Dr. Toshiyuki Nishimura (NIMS) for providing access to the evaluation of high-temperature strength, this study would not be as complete otherwise.

References

[1] M.M. Opeka, I.G. Talmy, J.A. Zaykoski, Oxidation-based materials selection for 2000°C + hypersonic aerosurfaces: Theoretical considerations and historical experience, J. Mater. Sci. 39 (2004) 5887–5904. https://doi.org/10.1023/B:JMSC.0000041686.21788.77.

[2] G.V. Samsonov, I.M. Vinitsky, Refractory Compounds. Handbook, Metallurgiya, Moscow, 1976. (in Russian)

[3] P.V. Zubarev, High-temperature strength of the interstitial phases, Metallurgiya, Moscow, 1985. (in Russian)

[4] T.Ya. Kosolapova, Properties, synthesis and application of refractory compounds. Reference Book, Metallurgiya, Moscow, 1986. (in Russian).

[5] R.A. Andrievskii, N.S. Strel'nikova, N.I. Poltoratskii, E.D. Kharkhardin, V.S. Smirnov, Melting point in systems ZrC-HfC, TaC-ZrC, TaC-HfC, Powder Metall Met Ceram 6 (1967) 65–67. https://doi.org/10.1007/BF00773385.

[6] O. Cedillos-Barraza, S. Grasso, N. Al Nasiri, D.D. Jayaseelan, M.J. Reece, W.E. Lee, Sintering behaviour, solid solution formation and characterisation of TaC, HfC and TaC–HfC fabricated by spark plasma sintering, J. Eur. Ceram. Soc. 36 [7] (2016) 1539–1548. https://doi.org/10.1016/j.jeurceramsoc.2016.02.009.

[7] D. Demirskyi, T.S. Suzuki, K. Yoshimi, O. Vasylkiv, Synthesis and high-temperature properties of medium-entropy (Ti,Ta,Zr,Nb)C using the spark plasma consolidation of carbide powders, Open Ceramics, 2 (2020) 100015. https://doi.org/10.1016/j.oceram.2020.100015.

[8] D. Demirskyi, T. Nishimura, T.S. Suzuki, Y. Sakka, O. Vasylkiv, K. Yoshimi, High-temperature toughening in ternary medium-entropy (Ta1/3Ti1/3Zr1/3)C carbide consolidated using spark-plasma sintering, J. Asian Ceram. Soc., 8[4] (2020) 1262–1270. https://doi.org/10.1080/21870764.2020.1840703.

[9] D. Demirskyi, H. Borodianska, T.S. Suzuki, Y. Sakka, K. Yoshimi, O. Vasylkiv, High-temperature flexural strength performance of ternary high-entropy carbide consolidated via spark plasma sintering of TaC, ZrC and NbC. Scr. Mater. 164 (2019) 12–16. https://doi.org/10.1016/j.scriptamat.2019.01.024.

[10] W.A. Sanders, H.B. Probst, High-temperature mechanical properties of polycrystalline hafnium carbide and hafnium carbide containing 13 vol.% hafnium diboride. Report NASA-TN-D-5008. NASA Lewis Research Centre, Cleveland, Ohio, 1963.

[11] W.A. Sanders, J.R. Creagh, C. Zalabak, J.J. Gangler, Preliminary investigation of the fabrication and properties of hafnium carbide, in: G.M. Ault, W.F. Barclay, H.P. Munger (Eds.), High-temperature material II, Interscience Publishers, N.Y., 1961, pp. 469–483.

Available via https://archive.org/details/nasa_techdoc_19630011490.

[12] Strength data of reference 634 in [4].

[13] L. Silvestroni, A.Bellosi, C. Melandri, D. Sciti, J.X. Liu, G.J. Zhang, Microstructure and properties of HfC and TaC-based ceramics obtained by ultrafine powder, J. Eur. Ceram. Soc. 31 [4] (2011) 619–627. https://doi.org/10.1016/j.jeurceramsoc.2010.10.036.

[14] D. Sciti, S. Guicciardi, M. Nygren, Densification and mechanical behaviour of HfC and HfB2 fabricated by spark plasma sintering, J. Am. Ceram. Soc. 91[5] (2008) 1433–1440. https://doi.org/10.1111/j.1551-2916.2007.02248.x.

[15] R.A. Andrievski, I.I. Spivak, Strength of Refractory Compounds, Metallurgiya, Chelyabinsk, 1989. (in Russian).

[16] H. Borodianska, D. Demirskyi, Y. Sakka, P. Badica, O. Vasylkiv, Grain boundary diffusion driven spark plasma sintering of nanocrystalline zirconia, Ceram. Int. 38 [5] (2012) 4385–4389. https://doi.org/10.1016/j.ceramint.2011.12.064.

[17] D. Demirskyi, O. Vasylkiv, Analysis of the high-temperature flexural strength behavior of B4C–TaB2 eutectic composites produced by in situ spark plasma sintering, Mater. Sci. Eng. A 697 (2017) 71–78. https://doi.org/10.1016/j.msea.2017.04.093.

[18] D. Demirskyi, O. Vaslykiv, Spark plasma sintering and high-temperature strength of B6O–TaB2 ceramics, J. Eur. Ceram. Soc. 37[8] (2017) 3009–3014. https://doi.org/10.1016/j.jeurceramsoc.2017.02.052.

[19] D. Demirskyi, Y. Sakka, O. Vasylkiv, High-Strength B4C–TaB2 Eutectic Composites Obtained via In Situ by Spark Plasma Sintering, J. Am. Ceram. Soc. 99 [7] (2016) 2436–2441. https://doi.org/10.1111/jace.14235.

[20] R. Darolia, T.F. Archbold, Plastic deformation of polycrystalline zirconium carbide, J. Mater. Sci. 11 (1976) 283–290. https://doi.org/10.1007/BF00551439.

[21] J. Schindelin, I. Arganda-Carreras, E. Frise, E. et al., Fiji: an open-source platform for biological-image analysis, Nat. Methods 9[7] (2012) 676–682. https://doi.org/10.1038/nmeth.2019.

[22] C. Zhang, A. Gupta, S. Seal, B. Boesl, A. Agarwal, Zhang Solid solution synthesis of tantalum carbide- hafnium carbide by spark plasma sintering. J. Am. Ceram. Soc. 100 [5] (2017) 1853–1862. https://doi.org/10.1111/jace.14778.

[23] O. Vasylkiv, H. Borodianska, Y. Sakka, D. Demirskyi, Flash spark plasma sintering of ultrafine yttria-stabilized zirconia ceramics, Scr. Mater. 121 (2016) 32–36. https://doi.org/10.1016/j.scriptamat.2016.04.031.

[24] T.K. Gupta, Instability of cylindrical voids in alumina, J. Am. Ceram. Soc. 61 [5-6] (1978) 191–195. https://doi.org/10.1111/j.1151-2916.1978.tb09276.x.

[25] S.-J. L. Kang, Sintering: Densification, Grain Growth and Microstructure, Elsevier Butterworth-Heinemann, Oxford, 2005.

[26] J.J. Fischer, Hot-pressing mixed carbides of Ta, Hf, and Zr, Am. Ceram. Soc. Bull. 43[3] (1964) 183–185.

[27] G.V. Samsonov, V.Y. Naumenko, L.N. Okhremchuk, Herstellung und Eigenschaften von Karbiden der Übergangsmetalle in ihren Homogenitätsbereichen, Phys. Status Solidi A 6[1] (1971) 201–211. https://doi.org/10.1002/pssa.2210060122.

[28] G.V. Samsonov, Yu.M. Goryachev, L.N. Okhremchuk, I.A. Podchernyaeva, V.S. Fomenko, Electron energy spectrum and physical properties of transition metal carbides in the region of homogeneity. Russ. Phys. J. 20[1] (1977) 30–36.

[29] G.V. Samsonov, V.N. Paderno, Preparation and properties of certain carbide alloys, Zh. Prikl. Khim. 36[12] (1963) 2759–2762.

[30] A.A. Ivanko, The Hardness, Naukova Dumka, Kyiv, 1968. (in Russian).

[31] R.B. Kotelnikov, S.N. Bashlykov, Z.G. Galiakbarov, A.I. Kashtanov, Extra refractory elements and compounds, Metallurgiya, Moscow, 1968. (in Russian).

[32] S.S. Ordan'yan, V.I. Unrod, A.E. Lutsenko, Reactions in the system HfC-HfB2, Innorg. Mater. 13 [3] (1977) 546–547.

[33] R.W. Rice, Porosity of Ceramics: Properties and Applications, Marcel Dekker, New York, 1998.

[34] E. Wuchina, M. Opeka, S. Causey, K. Buesking, J. Spain, A. Cull, J. Routbort, F. Gutierrez-More, Designing for ultrahigh-temperature applications: The mechanical and thermal properties of HfB2, HfC x , HfN x and αHf(N). J. Mate. Sci. 39 (2004) 5939–5949. https://doi.org/10.1023/B:JMSC.0000041690.06117.34.

[35] G.G. Travuskin, V.I. Knyazev, V.S. Belov, G.A. Rymashevskii, Temperature threshold of brittle failure in interstitial phases, Strength Mater. 5 (1973) 639–641. https://doi.org/10.1007/BF00762329.

[36] V.M. Baranov, V.I. Knyazev, O.S. Korostin, The temperature dependence of the elastic constants of nonstoichiometric zirconium carbides, Strength Mater. 5 (1973) 1074–1077. https://doi.org/10.1007/BF00762754.

[37] D. Kalish, E.V. Clougherty, K. Kreder, Strength, Fracture Mode, and Thermal Stress Resistance of HfB2 and ZrB2, J. Am. Ceram. Soc. 52 [1] (1969) 30–36. https://doi.org/10.1111/j.1151-2916.1969.tb12655.x.

[38] A. Kelly, D.J. Rowcliffe, Deformation of polycrystalline transition metal carbides, J. Am. Ceram. Soc. 50 (1967) 253–256. https://doi.org/10.1111/j.1151-2916.1967.tb15098.x.

[39] Data of reference 14 cited by [20]. J.L. Martin, P. Gayet, P. Costa, Stress changes in tantalum carbide with the deformation rate and temperature (1200 and 2200C), Compt. Rend. Ser. C. 272 [26] (1971) 2127–2130.

[40] G.V. Samsonov, Interaction between carbon and refractory metals, Metallurgiya, Moscow, 1974. (in Russian)

[41] R.A. Andrievsky, V.V. Klymentko, Y.F. Khromov, Self-diffusion of carbon in transition metal carbides of IV and V group, Phys. Met. Metallogr. 28 [2] (1969) 298–303.

[42] V.N. Zagryazkin, On mechanism of diffusion in monocarbides of transition metals, Phys. Met. Metallogr. 28 [2] (1969) 292–297.

[43] R.M. Spriggs, T. Vasilos, Effect of Grain Size on Transverse Bend Strength of Alumina and Magnesia, J. Am. Ceram. Soc. 46 [5] (1963) 224–228. https://doi.org/10.1111/j.1151-2916.1963.tb19777.x.

[44] R.F. Canon, J.T.A. Roberts, R.J. Beals, Canon Deformation of UO2 at High Temperatures, J. Am. Ceram. Soc. 54 [2] (1971) 105–112. https://doi.org/10.1111/j.1151-2916.1971.tb12230.x.

[45] R.L. Coble, A Model for Boundary Diffusion Controlled Creep in Polycrystalline Materials, J. Appl. Phys. 34 (1963) 1679–1682. https://doi.org/10.1063/1.1702656.

[46] S.M. Katz, S.S. Ordan'yan, G.P. Zaitsev, High-temperature creep in solid-solutions of the HfC–TaC system, Izd. Akad. Nauk SSSR, Neorg. Mat. 17[11] (1981) 2039–2043.

[47] S.M. Katz, S.S. Ordan'yan, A.I. Goryn, S.S. Semenov, L.V. Kudryasheva, Effect of WC on creep of zirconium carbide, Izd. Akad. Nauk SSSR, Neorg. Mat. 15[10] (1971) 1775–1778.

[48] A.I. Avgustinik, S.M. Katz, S.S. Ordan'yan, A.I. Goryn, L.V. Kudryasheva, Compressive creep in ZrC–NbC solid-solutions at temperatures 2600–3150°K, Izd. Akad. Nauk SSSR, Neorg. Mat, 7[8] (1972) 1417–1420.

Tables

Table 1 Creep and diffusion data by various methods for HfC and ZrC

System	Method	Qa, kJ/mol	Temperature range, °C	Reference
^{14}C in HfC	Isotope tracing	545±54	2200–2800	[41]
^{14}C in α-Hf	Isotope tracing	312	1120–1760	[40]
^{14}C in β-Hf	Isotope tracing	167	1820–2130	[40]
Hf in HfC	Diffusion theory	764	-	[42]
HfC0.98	Compressive creep	833[*1]	2400– 2700	[3]
ZrC0.94	Compressive creep	678[*1]	2200–2600	[3]
ZrC0.93	Tensile creep	720[*2]	2200–2400	[3]
ZrC0.98	Creep in flexure	368[*3]	1800–2200	[3]
ZrC0.94	Flexure	501±19[*3]	1600–1800	[20]
HfC0.99	Flexure	370±15	1800–2000	This study

The mechanism identified by authors of the original study (ref. [3]) is presented:

[*1] Creep controlled by bulk diffusion of Me in carbide

[*2] Dislocation-driven creep controlled by bulk diffusion of C in carbide

[*3] Dislocation glide controlled by bulk diffusion of C in carbide

Figure captions

Figure 1. X-ray diffraction patterns of initial powder and hafnium carbide bulk consolidated at 2000 °C. Lattice parameters are 4.6399 Å and 4.6414 Å for powder and bulk ceramic, respectively. Inset shows details of the (440) peak.

Figure 2. X-ray diffraction pattern and Rietveld refinement of hafnium carbide bulk. Inset shows details of the (440) peak.

Figure 3. Evaluation of theoretical density for fully bulk specimens according to SEM analysis (>98%). Bulk density represents a mean value of five measurements. SEM analysis was performed at magnification of ×500. Up to 4 microstructures were analyzed for every point.

Figure 4. Competition between density and grain growth for the hafnium carbide during the consolidation process using spark-plasma sintering at 1600–2000 °C. Four ceramics grades selected for high-temperature tests were consolidated using 25 or 30 mm diameter dies.

Figure 5. Microstructure evolution during consolidation of hafnium carbide. Note that the density of the specimen increases from left to right. Results of a pretrained automatic microstructure segmentation application are provided below the original SEM. SEM images were obtained at identical magnification using the BSE mode. Black or dark-grey inclusions in BSE images are pores or grain pull-outs.

Figure 6. SEM micrographs of selected hafnium carbide ceramics: (a,b) Grade A, (c,d) Grade B, (e,f) Grade C, and (g,h) Grade D. All images are taken in the BSE mode. (a,c,e,g) show polished surface, while (b,d,f,h) show fracture after 2000 °C tests. Identical magnification was used for the polished and fractured specimens. Arrows in (g) show the location of oxide phase.

Figure 7. Effect of loading force on hardness of hafnium carbide bulks. Data from previous studies contained mainly microhardness [2,4,27–32], only refs [13,22,6] reported hardness at load of 9.8 N.

Figure 8. Hall-Petch-like relation for hafnium carbide ceramics with a density exceeding 98% TD following tests at ambient temperature. Open squares are data from ref [13].

Figure 9. Young's modulus of hafnium carbide at ambient temperature as a function of porosity.

Figure 10. Young's modulus of hafnium carbide at elevated temperature for highly-dense specimens.

Figure 11. Effect of temperature on flexural strength of monolithic hafnium carbide ceramics [10–13]. Closed symbols indicate that the strength was measured using a four-point setup and the open symbols show the results of the three-point flexural strength tests. Note that the high-temperature strength of grade D showed no dependence on the loading rate. Thus flexural strength obtained using loading rate

of 0.5 mm/min is provided for grades A and B. Data for grade C and D overlapped within the error of measurements.

Figure 12. Effect of temperature and strain rate on the yield stress for HfC grade A during flexural tests at 1800 °C –2000 °C. (b) and (c) shows typical strain-stress curves for different strain rates at 1800°C and 2000 °C, respectively. Numbers here are the strain rate using during the flexural test in s^{-1}. There was an initial loading effect present in all strain-stress curves due to the accommodation of rollers during the flexural test.

Figure 13. The variation in the yield stress of HfC grade D with the strain at 1800 °C and 2000 °C. Data for grade B at 1800 °C are provided as a reference.

Figure 14. The variation in the yield stress of HfC grade B with the plastic strain at 1800 °C and 2000 °C. Data for zirconium carbide was approximated using the data from ref [20].

Figure 15. Effect of temperature on fracture of hafnium carbide grade D: (a) 25 °C, (b) 1600 °C, (c) 1800 °C, (d) 1900 °C and (e) 2000 °C. All images were acquired in the BSE mode from the center of the bar after flexure. The bulk density of specimens was 12.392 g/cm^3, and mean grain size of 78±34 μm.

Figures

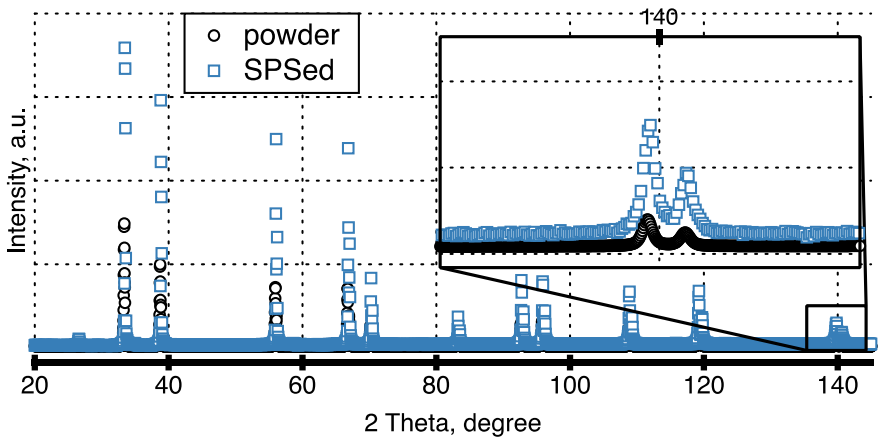

Figure 1. X-ray diffraction patterns of initial powder and hafnium carbide bulk consolidated at 2000 °C. Lattice parameters are 4.6399 Å and 4.6414 Å for powder and bulk ceramic, respectively. Inset shows details of the (440) peak.

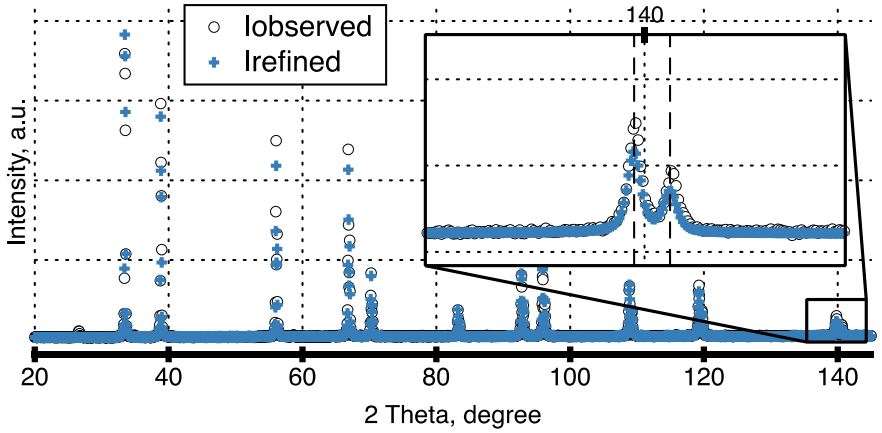

Figure 2. X-ray diffraction pattern and Rietveld refinement of hafnium carbide bulk. Inset shows details of the (440) peak.

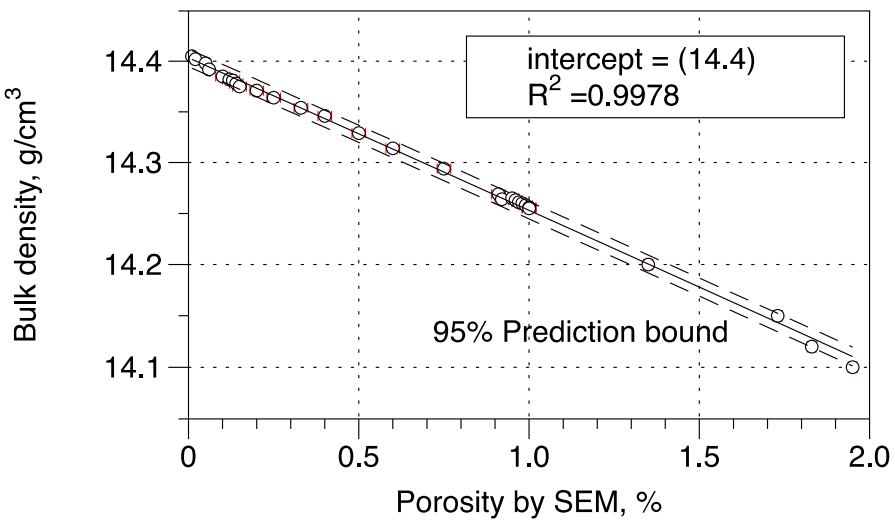

Figure 3. Evaluation of theoretical density for fully bulk specimens according to SEM analysis (>98%). Bulk density represents a mean value of five measurements. SEM analysis was performed at magnification of ×500. Up to 4 microstructures were analyzed for every point.

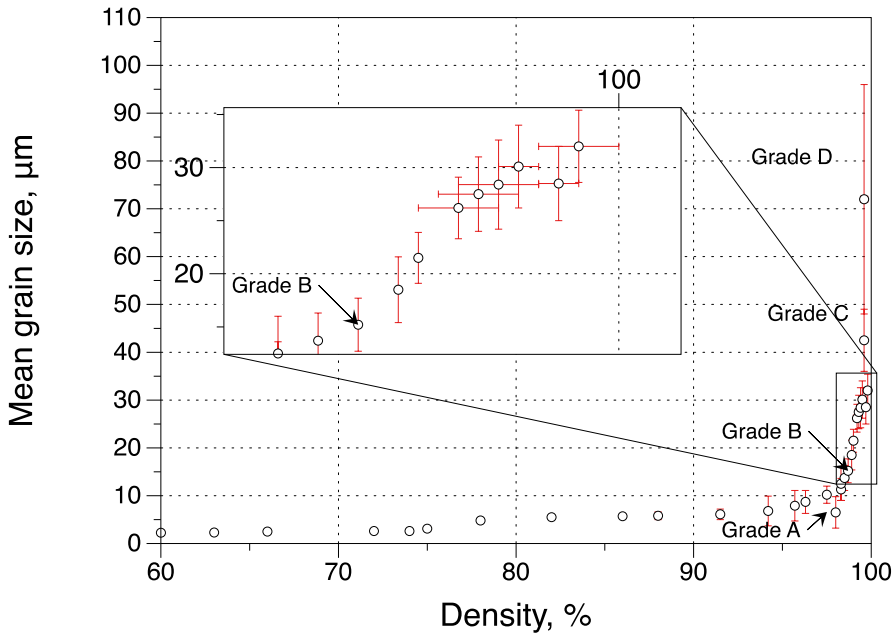

Figure 4. Competition between density and grain growth for the hafnium carbide during the consolidation process using spark-plasma sintering at 1600–2000 °C. Four ceramics grades selected for high-temperature tests were consolidated using 25 or 30 mm diameter dies.

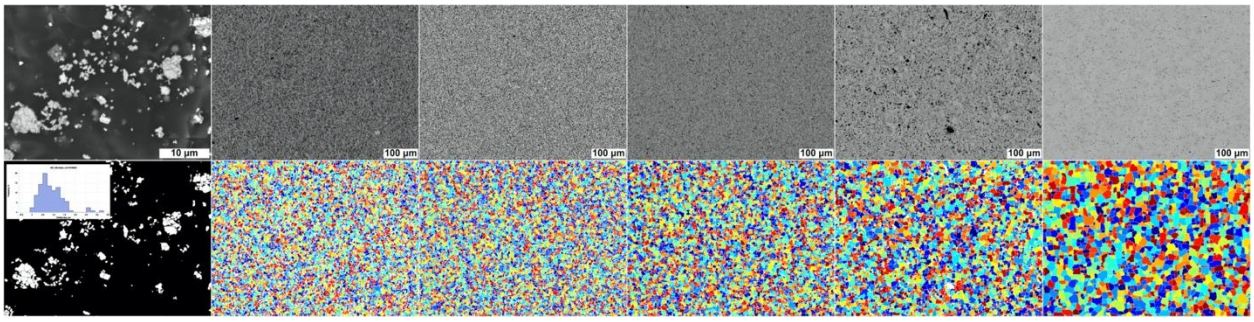

Figure 5. Microstructure evolution during consolidation of hafnium carbide. Note that the density of the specimen increases from left to right. Results of a pretrained automatic microstructure segmentation application are provided below the original

SEM. SEM images were obtained at identical magnification using the BSE mode. Black or dark-grey inclusions in BSE images are pores or grain pull-outs.

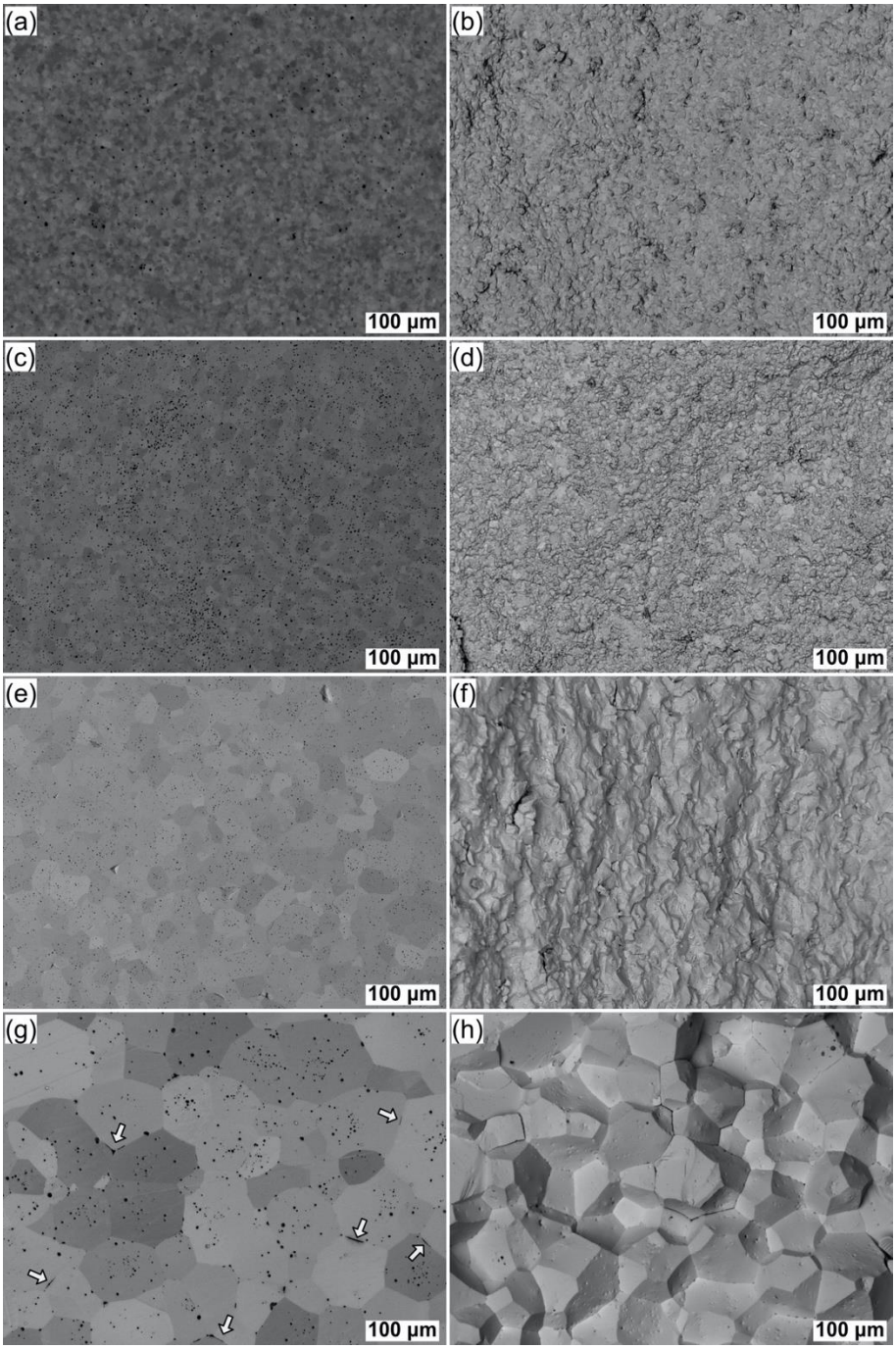

Figure 6. SEM micrographs of selected hafnium carbide ceramics: (a,b) Grade A, (c,d) Grade B, (e,f) Grade C, and (g,h) Grade D. All images are taken in the BSE

mode. (a,c,e,g) show polished surface, while (b,d,f,h) show fracture after 2000 °C tests. Identical magnification was used for the polished and fractured specimens. Arrows in (g) show the location of oxide phase.

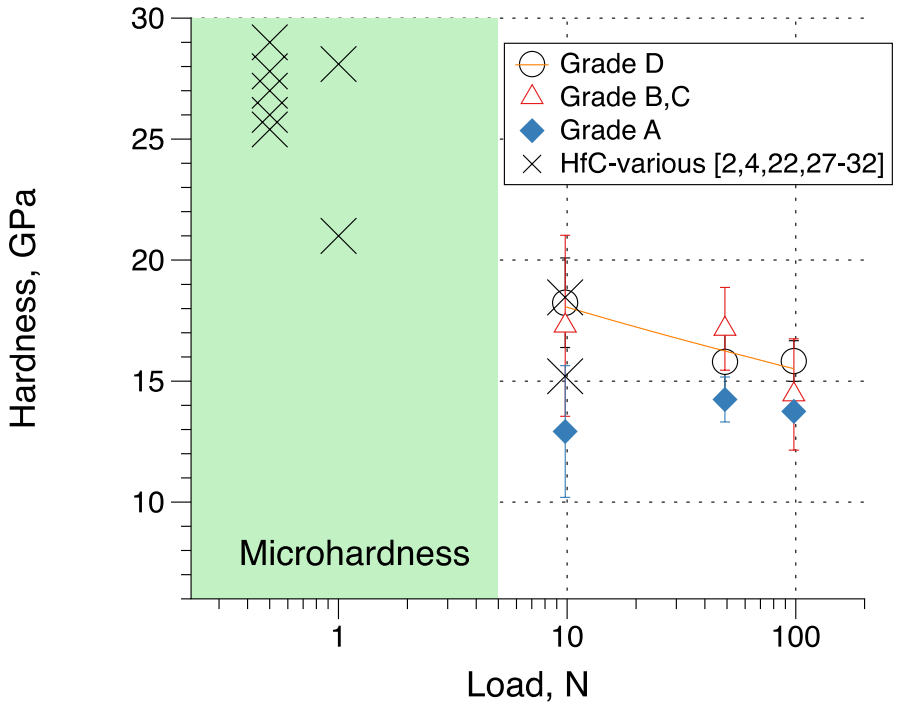

Figure 7. Effect of loading force on hardness of hafnium carbide bulks. Data from previous studies contained mainly microhardness [2,4,27–32], only refs [13,22,6] reported hardness at load of 9.8 N.

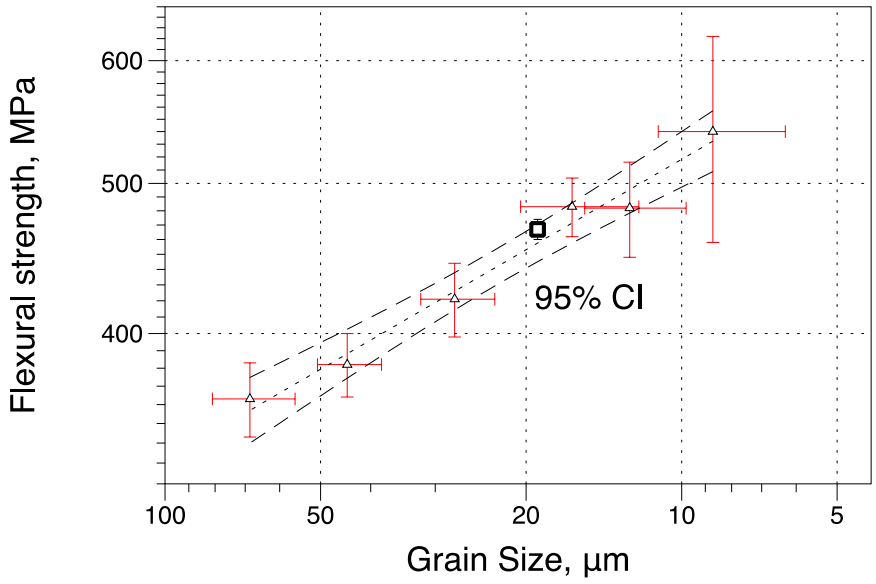

Figure 8. Hall-Petch-like relation for hafnium carbide ceramics with a density exceeding 98% TD following tests at ambient temperature. Open squares are data from ref [13].

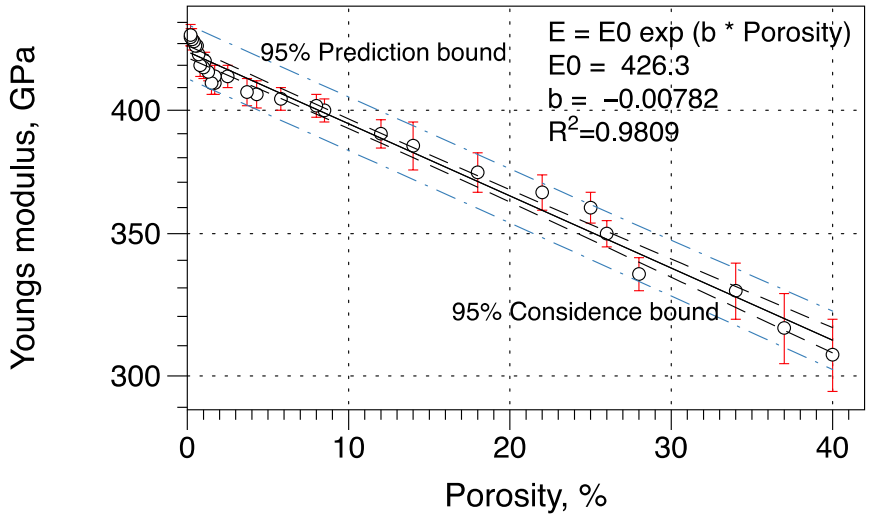

Figure 9. Young's modulus of hafnium carbide at ambient temperature as a function of porosity.

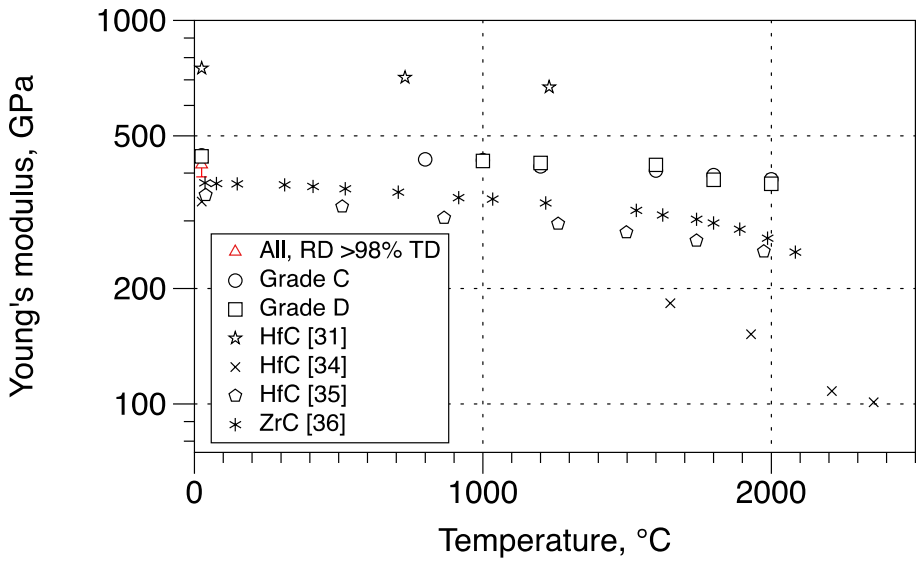

Figure 10. Young's modulus of hafnium carbide at elevated temperature for highly-dense specimens.

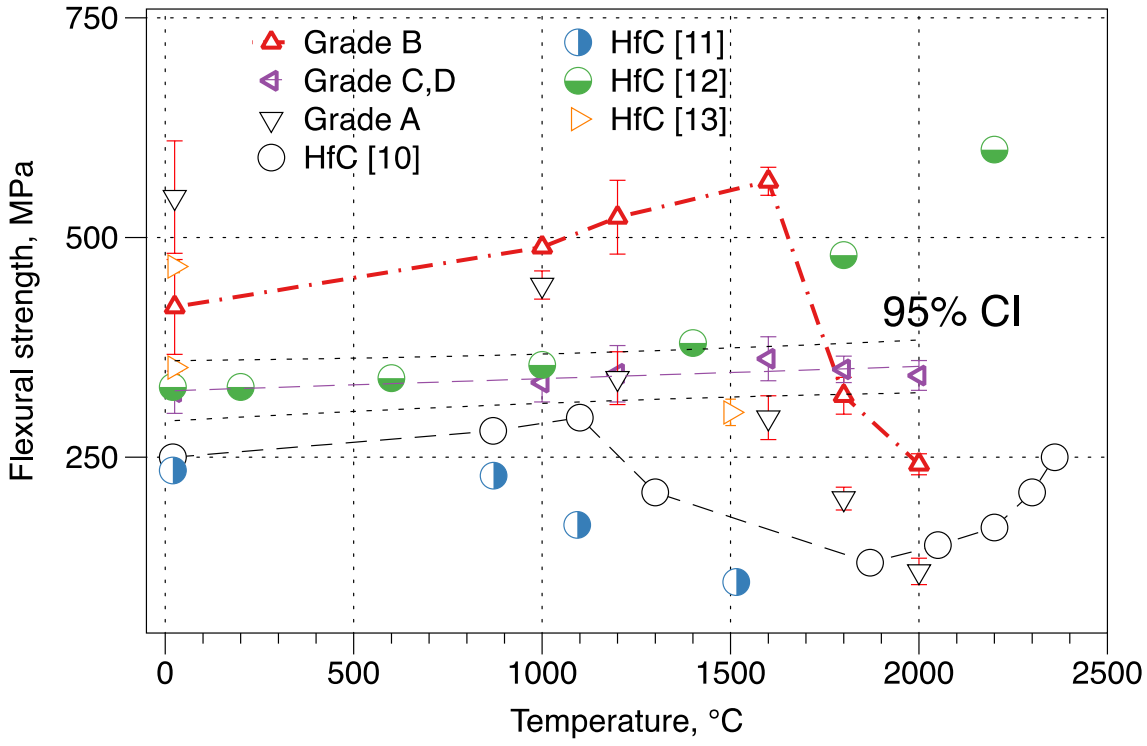

Figure 11. Effect of temperature on flexural strength of monolithic hafnium carbide ceramics [10–13]. Closed symbols indicate that the strength was measured using a

four-point setup and the open symbols show the results of the three-point flexural strength tests. Note that the high-temperature strength of grade D showed no dependence on the loading rate. Thus flexural strength obtained using loading rate of 0.5 mm/min is provided for grades A and B. Data for grade C and D overlapped within the error of measurements.

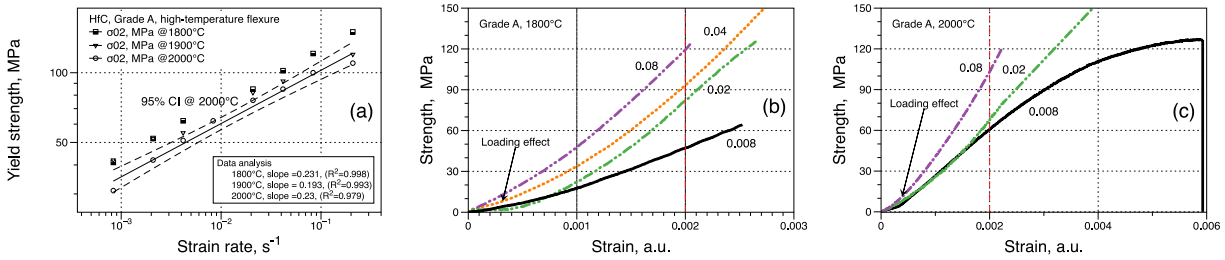

Figure 12. Effect of temperature and strain rate on the yield stress for HfC grade A during flexural tests at 1800 °C –2000 °C. (b) and (c) show typical strain-stress curves for different strain rates at 1800°C and 2000 °C, respectively. Numbers here are the strain rate using during the flexural test in s^{-1}. There was an initial loading effect present in all strain-stress curves due to the accommodation of rollers during the flexural test.

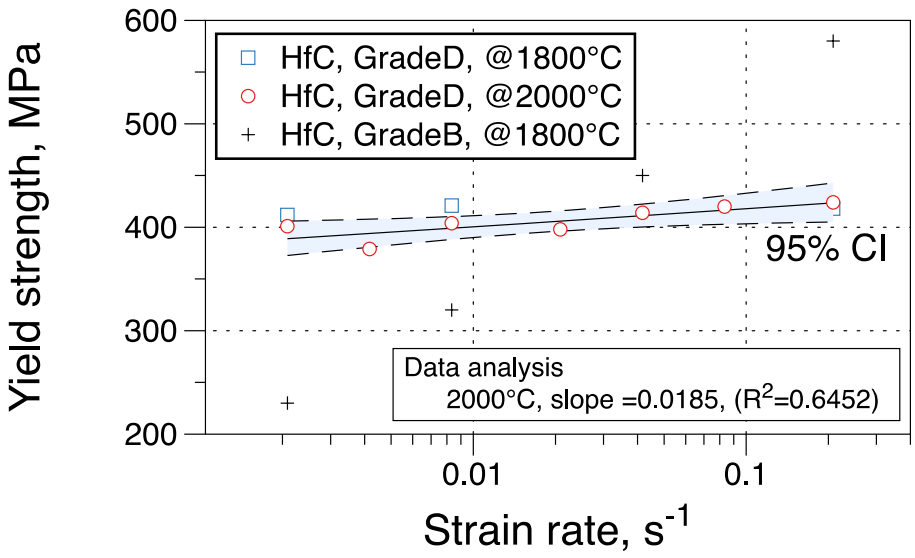

Figure 13. The variation in the yield stress of HfC grade D with the strain at 1800 °C and 2000 °C. Data for grade B at 1800 °C are provided as a reference.

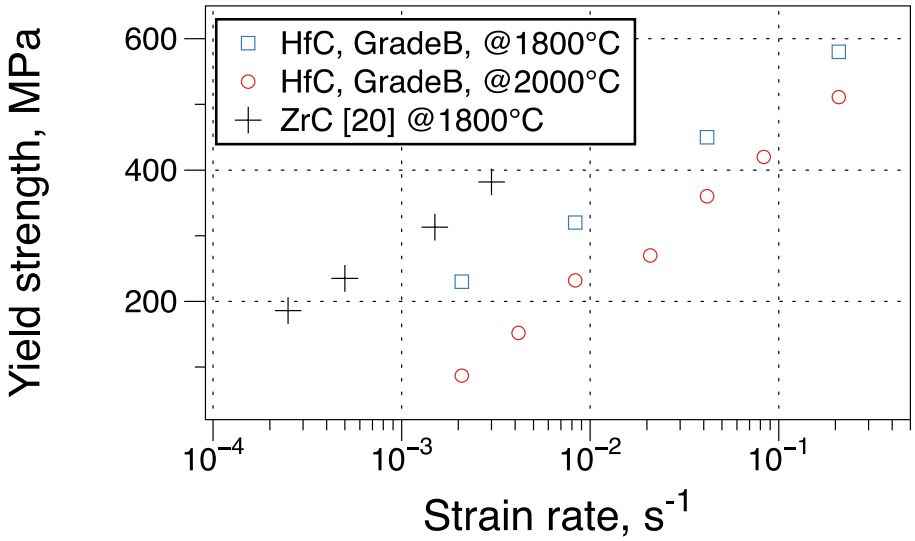

Figure 14. The variation in the yield stress of HfC grade B with the plastic strain at 1800 °C and 2000 °C. Data for zirconium carbide was approximated using the data from ref [20].

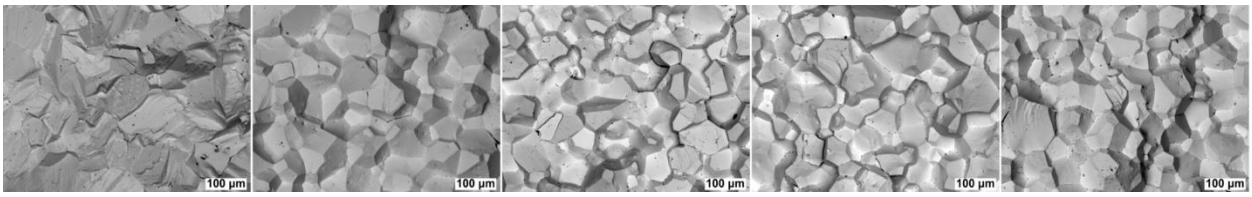

Figure 15. Effect of temperature on fracture of hafnium carbide grade D: (a) 25 °C, (b) 1600 °C, (c) 1800 °C, (d) 1900 °C and (e) 2000 °C. All images were acquired in the BSE mode from the center of the bar after flexure. The bulk density of specimens was 12.392 g/cm^3, and mean grain size of 78±34 µm.

Declaration of interests

☒ The authors declare that they have no known competing financial interests or personal relationships that could have appeared to influence the work reported in this paper.

☐The authors declare the following financial interests/personal relationships which may be considered as potential competing interests: